

## Supporting Information

### **Nanoscaled self-alignment of Fe<sub>3</sub>O<sub>4</sub> nanodisc in ultrathin rGO film with engineered conductivity for electromagnetic interference shielding**

*Yong Yang<sup>a</sup>, Meng Li<sup>b\*</sup>, Yuping Wu<sup>a</sup>, Tao Wang<sup>c</sup>, Eugene Shi Guang Choo<sup>d</sup>, Jun Ding<sup>b</sup>, Baoyu Zong<sup>a</sup>, Zhihong Yang<sup>a</sup> and Junmin Xue<sup>b\*</sup>*

<sup>a</sup> Temasek Laboratories, National University of Singapore, 5A Engineering Drive 1, Singapore 117411

<sup>b</sup> Department of Materials Science and Engineering, National University of Singapore, 117574, Singapore.

Email: [mseimg@nus.edu.sg](mailto:mseimg@nus.edu.sg) (Dr. M. Li); [msexuejm@nus.edu.sg](mailto:msexuejm@nus.edu.sg) (Prof. J. Xue)

<sup>c</sup> Key Laboratory for Magnetism and Magnetic Materials of the Ministry of Education, Lanzhou University, Lanzhou 730000, People's Republic of China

<sup>d</sup> Carl Zeiss Pte. Ltd., Microscopy Business Group, Singapore, 415926

*Yong Yang and Meng Li contributed equally to this work.*

***Detailed procedure of filtration:*** In the filtration assisted self-assembly process, mixed cellulose ester filter membrane (pore size of 200 nm) was used the primary filter layer and normal filter paper (pore size around 2  $\mu\text{m}$ ) was placed in the bottom as secondary protective layer. It is recommended to use the miniwatt vacuum pump with relatively less suction in order to provide enough self-assembly duration. Additionally, it is noted that the diameter of filter papers should be larger than that of suspension container on the upper layer (details can be found in our previous work<sup>1</sup>) in order to facilitate peeling off the film from the filter paper. In the first step, little amount of pure GO suspensions were dropped into suspension container to just cover filter membrane. The filtration process is further retarded due to the capillary pressure between GO sheets on the filter membrane. After few minutes, little amount of GO@ $\alpha\text{-Fe}_2\text{O}_3$  nanodisc suspension was subsequently dropped into the container in the flowing steps, and the slow filtration process provide enough duration for iron oxide nanoparticles to be mono-dispersed and self-assemble in-between GO layers. The whole process normally take several hours. After finishing the self-assembled filtration process, the hybrid film was kept on the filter membrane for another few hours before carefully peeling off. The nanodisc loading fraction can be adjusted by controlling the volume of  $\alpha\text{-Fe}_2\text{O}_3$  nanodisc aqueous (1 mg/ml). In the second step, the hybrid films were annealed at 420 °C for 2 hour under under 5%  $\text{H}_2$  and 95% Ar atmosphere. The thickness of the films can be controlled by adjusting the concentration or the volume of the aqueous suspension. All the samples mass were determined by weighting the films vacuum dried at 80 °C for 12 hours. The thickness of the films was measured with five independence slices and the average values were used to calculate the volume. The same filtration procedure is adopted to fabricate rGO/ $\text{Fe}_3\text{O}_4$  nanosphere.

***FIB imaging:*** The notch cross-section was prepared by focused ion beam (FIB) milling using AURIGA 60 FIB-SEM Crossbeam (Carl Zeiss Microscopy GmbH, Germany). Prior to milling, the top surface of the material was protected with ~100 nm layer of Pt metal induced by e-beam assisted gas deposition, followed by ~400 nm layer of Pt induced by ion-beam assisted gas deposition. Using a 30 kV; 4nA focused ion beam (FIB) current a coarse incision was milled directly into the surface of the material in order to achieve a viewing channel for the SEM imaging. The notch of about 5  $\mu\text{m}$  wide was fine polished using a 30 kV: 50 pA FIB probe current. The cross-section face was imaged using the 30 $\mu\text{m}$  aperture at 1 kV accelerating voltage, and the In-lens secondary electron and energy-selective backscatter detectors.

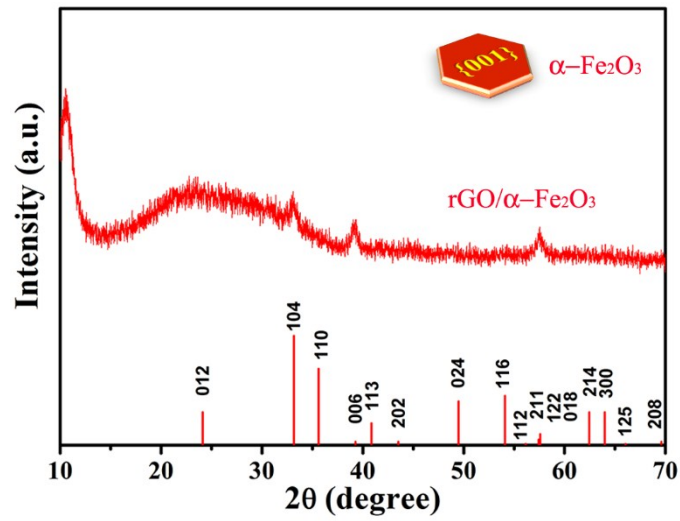


Fig. S1. XRD spectrum of GO/ $\alpha$ -Fe<sub>2</sub>O<sub>3</sub> nanodisc hybrid film. The standard spectrum of  $\alpha$ -Fe<sub>2</sub>O<sub>3</sub> (JCPDS#33-0664) is provided for comparison. The inset illustrates the {001} basal plane of the  $\alpha$ -Fe<sub>2</sub>O<sub>3</sub> nanodisc.

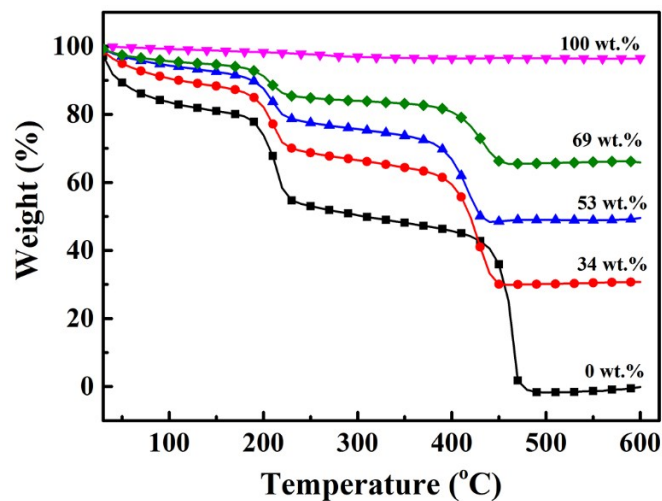


Fig. S2. TGA weight loss curves of rGO/Fe<sub>3</sub>O<sub>4</sub> nanodisc hybrid films with different loading weight fractions. The weight reduction occurring around 200 °C could be attributed to the pyrolysis of the labile oxygen-containing groups in the form of CO, CO<sub>2</sub> and steam. This weight reduction has been deducted when calculating the weight fraction of Fe<sub>3</sub>O<sub>4</sub> nanodisc in each hybrid film.<sup>2-4</sup>

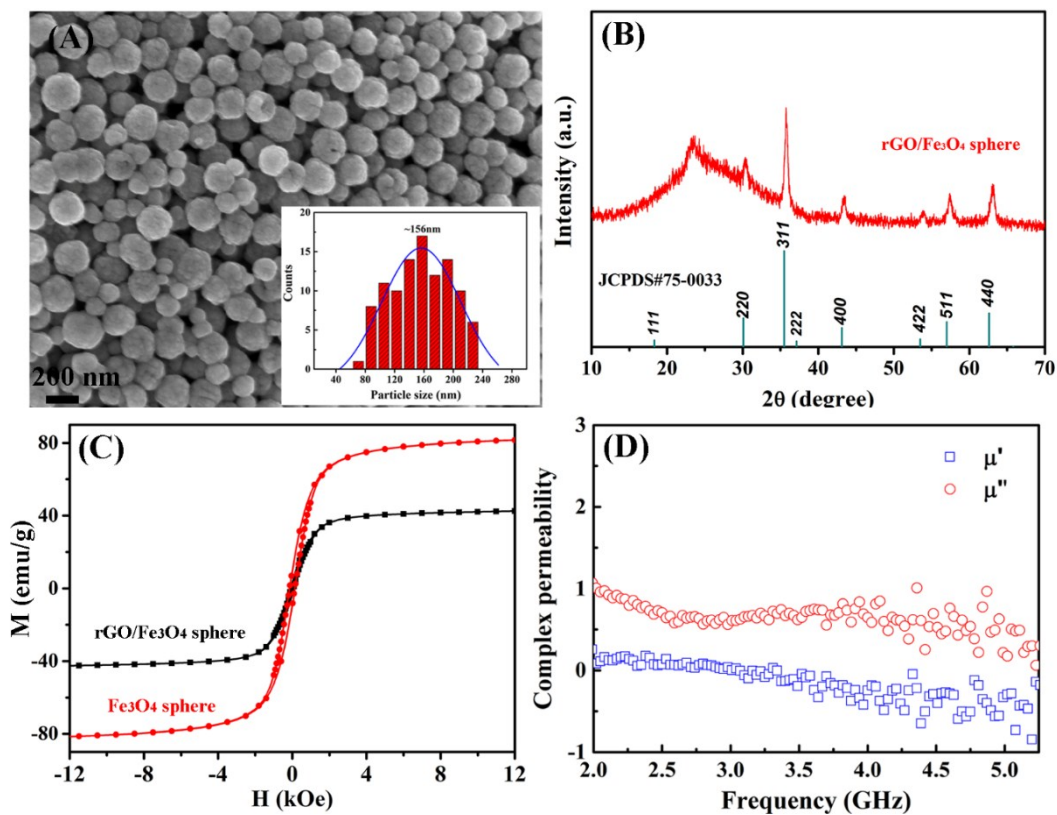


Fig. S3. (A) SEM image  $\text{Fe}_3\text{O}_4$  nanospheres. The inset shows the size distribution. (B) XRD pattern of  $\text{rGO}/\text{Fe}_3\text{O}_4$  nanosphere hybrid paper. (C) Hysteresis loops of the nanosphere and the hybrid paper. (D) Complex permeability of the hybrid paper measured in 2.0-5.2 GHz.

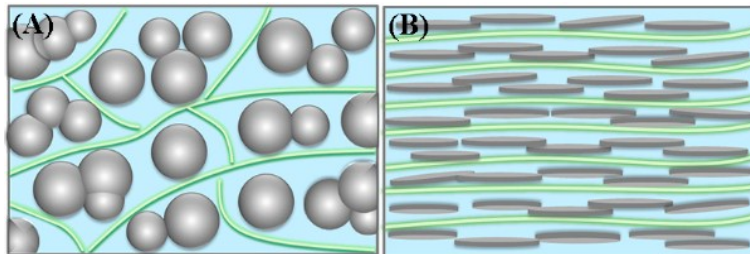


Fig. S4. Illustration of microstructure of rGO hybrid film embedded with (A) spherical nanoparticles and (B) nanodiscs. The green line represents the conducting network of rGO sheets.

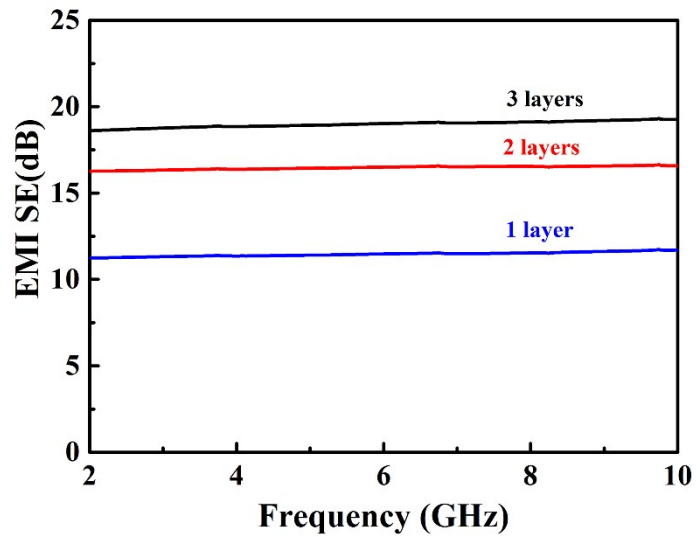


Fig. S5. Frequency dependent EMI SE of multilayer rGO/Fe<sub>3</sub>O<sub>4</sub> nanodisc hybrid films.

## Supporting Information References

1. M. Li, Z. Tang, M. Leng and J. Xue, *Adv. Funct. Mater.*, 2014, **24**, 7495.
2. J. Shen, Y. Hu, M. Shi, X. Lu, C. Qin, C. Li and M. Ye, *Chem. Mater.*, 2009, **21**, 3514-3520.
3. Y. Zhang, H.-L. Ma, Q. Zhang, J. Peng, J. Li, M. Zhai and Z.-Z. Yu, *J. Mater. Chem.*, 2012, **22**, 13064-13069.
4. C. Liu, F. Hao, X. Zhao, Q. Zhao, S. Luo and H. Lin, *Sci. Rep.*, 2014, **4**, 3965.